Received: 22 February 2022 | Revised: 18 May 2022 | Accepted: 28 June 2022

DOI: 10.1002/suco.202200181

ARTICLE

fib CEB-FIP WILEY

Experimental methods for the analysis of the tensile behavior of concrete joints

Jan P. Höffgen[1] | **Matthias Mohs**[1,2] | **Eric Sonderegger**[1] | **Viktória Malárics-Pfaff**[2] | **Frank Dehn**[1]

[1]Karlsruhe Institute of Technology, Institute of Concrete Structures and Building Materials, Karlsruhe, Germany

[2]Federal Waterways Engineering and Research Facility, Structural Engineering, Karlsruhe, Germany

Correspondence
Jan P. Höffgen, Karlsruhe Institute of Technology, Institute of Concrete Structures and Building Materials, Gotthard-Franz-Str. 3, Karlsruhe, 76131, Germany.
Email: hoeffgen@kit.edu

Abstract

Adhesion plays an important role in the evaluation of hydraulic structures with unreinforced concrete joints. The experimental determination of joint tensile strength as a quantifiable parameter is not standardized, resulting in a variety of test setups found in literature. The present paper highlights advantages and disadvantages of three of the most common tension tests for plain concrete and concrete joints through both theoretical and laboratory experimental analysis on specimens with artificial joints. Splitting tension tests were found to be inexpensive but tend to overestimate the adhesive strength of weak joints. Direct tension tests require an elaborate test setup but may yield information on the tension softening behavior. Pull-off tests stand out for their ability to yield in-situ results but deliver inconclusive results.

KEYWORDS

adhesion, direct tension test, fracture energy, joint, plain concrete, pull-off test, splitting test, tension

1 | INTRODUCTION

Hydraulic structures are exposed to high stresses resulting mainly from horizontal loads from earth and water pressure. Consequently, in the joints of unreinforced hydraulic structures, such as locks, weirs, and dams, shear-friction and adhesion are the major load-transfer mechanisms. Unlike shear friction, adhesion does not require normal loads or shear deformation. Therefore, adhesion can be regarded as the resistance against cracking prior to a subsequent shearing-off of interfaces. The characterization of adhesion through the tensile behavior can only be considered an auxiliary approach as part of a structural integrity analysis, since failure of adhesion in hydraulic structures is rarely caused by external tensile forces but rather by environmental impacts or weathering in combination with shear-fatigue. However, the evaluation of existing concrete structures with concrete joints requires validated setups for assessing the interfacial tensile strength.

There are several methods for the experimental investigation of the tensile resistance of plain concrete, distinguishing direct tension, where a tensile force is applied to a specimen, and indirect tension, where tensile stresses are the result of external compressive forces.

Discussion on this paper must be submitted within two months of the print publication. The discussion will then be published in print, along with the authors' closure, if any, approximately nine months after the print publication.

Direct tension tests require specialized setups, due to the brittleness or concrete. In order to ensure that the applied tensile load is initiated evenly onto the specimens, and further, to prevent the emergence of moments due to a possible twisting, specimens need to be glued directly to the test machine. Otherwise, both effects would strongly reduce the tensile-bearing capacity. Alternatively, bone-shaped specimens may be clamped into test machines, which limit specimen geometry. In addition to the tensile strength, specialized setups with high stiffness and fixed load application allow the measurement of tension softening curves, from which fracture energy can be derived.[1,2]

The most common indirect tension test is the splining tension test, or Brazilian test, which uses a standard compressive test setup and yields tensile stresses that are rather similar to the uniaxial tensile strength.[3] An adaption, the wedge-splitting test, can be used to calculate fracture energy.[4–7] Alternatively, the flexural strength obtained from bending tests can be converted into the tensile strength through assumptions of stress distribution. Flexural tests can also serve for the determination of fracture energy.[8] Conversion formulae for various indirect tension tests have been experimentally and numerically investigated, but remain disputed.

The tensile strength of concrete joints is much lower than the monolithic concrete tensile strength. Joint tensile strength is influenced by a variety of parameters, including the surface preparation method, achieved interfacial roughness, and concrete flow characteristics.[6,7]

All tension test setups can be adapted for the measurement of the tensile behavior of concrete joints. Flexural tests, however, are rarely used.[9–11] The most common indirect tension tests for determining the tensile bond strength is the splitting tension test, which can be performed on cylindrical or prismatic specimens.[6,12–17] The former, however, present a problem with aligning joint interface and load application. This is facilitated when testing prismatic specimens for the predetermination of the crack path through both joint interface and testing method is favorable. Since splitting tension tests are problematic for their nonuniform stress distribution, results for joint tensile strength must be regarded with caution, as joints introduce a discontinuity, which may further influence cracking.

Direct tension tests can be performed without adaption of the test setup. Testing on joints even proves beneficial for the determination of the tensile bond strength, as the structural weakness introduced by the joint may locate cracking and thereby facilitates load application and reduces the need for notches. Thus, in contrast to monolithic concrete, bond tensile strength and fracture energy can be determined on the same specimen. However, the reduced crack interlocking increases the magnitude of snap-back effects.

An adapted form of the direct tension test is the pull-off test, which was developed for the in-situ assessment of the adhesive bond between concrete and overlays and can also be used for laboratory tests of concrete-to-concrete joint tensile strength.[13,16,18–20] Results, however, are heavily influenced by the test realization, as the partial drilling of cores may lead to damaged interface or load eccentricities. The exact alignment of the drill-cores and the testing device as well as the perpendicularity to the joint are important for the reliability of the results. Measured results found in literature often do not represent the actual bond tensile strength but a minimal value when instead of the interface cracking occurs in the surrounding material.[21] This might be sufficient for in-situ quality assessment of concrete repair or retrofitting, but impedes scientific analyses. Nonetheless, due to the simple test setup, the pull-off tests remains a popular method. Studies show pull-off test yield similar or marginally lower joint bond tensile strengths than splitting tension tests.[13,16]

In this paper, three experimental methods to determine the adhesive bond strength of concrete joints are analyzed: the splitting tension test, which is the most common indirect tension test method, the laboratory direct tension test, which can deliver several material parameters without requiring stress conversion, and the pull-off test, which is standardized for the in-situ testing of concrete interfaces. While all specimens were produced in a similar manner and with the same concrete mix design, the presented results focus on highlighting individual benefits and shortcomings of the methods within themselves.

2 | MATERIALS AND SPECIMENS PREPARATION

Specimens for the experimental analysis were produced in seven casting batches. Table 1 shows the adopted mix design. Aggregates were quartzitic Rhine sand and Rhine gravel with AB 16 as grading curve. CEM I 32.5 R was used as binder with a water/cement-ratio of w/c = 0.57.

Four different joint roughening methods were adopted: as-cast (a), where joints were left untreated after smoothing with a trowel, raked (r), treated approximately 6 h after mixing when hardening had begun, as well as steel-wire-brushed (b) and water-jetted (w), performed 24 h after casting. With the exception of raked interfaces, which showed a distinguished pattern, the treatment methods resulted in superficial roughening, as illustrated in Figure 1. Joints were generally produced horizontally

at medium specimen height with the exception of pull-off tests, where the thickness of the overlay was 50 mm (Figure 2). Following demolding 1 day after mixing, specimens were stored in a climatic room at 20°C and 100% r. h. until the addition of the second concrete layer at the age of 7 days. At the same step, additional monolithic (m) reference specimens without joints were produced. The completed specimens were stored at 20°C and 100% r. h. for 7 days and at 65% r. h. for the following 21 days until testing.

For each of the seven batches, the compressive strength of monolithic cubes ($l = 150$ mm) at the age of 28 days was measured, yielding $f_{cm,cube} = 41.8$ MPa in average, according to EN 12390-3:2019-10.[22] Additionally, cylinders of the first and last batch ($d = 150$ mm, $h = 300$ mm) were used to determine splitting tensile strength $f_{ctm,sp} = 3.0$ MPa, compressive strength $f_{cm} = 39.4$ MPa, and compressive secant modulus $E_{cm,S} = 29.9$ GPa.

TABLE 1 Mix design for laboratory analysis

		Proportion [kg/m³]
Sand	0–2 mm	701.8
Gravel	2–8 mm	379.4
Gravel	8–16 mm	815.6
CEM I 32.5 R		310.0
Water		176.7

3 | SPLITTING TENSION TESTS

To determine the cohesion (i.e., the tensile strength of bulk concrete without joints) and adhesion (i.e., the tensile strength of the interface) properties of construction joints, splitting tension tests according to EN 12390-6:2010-09[23] were carried out. The great advantage of splitting tension tests is the simplicity of the implementation and the test setup. In addition, the position of the maximum tensile stress in the sample can be approximately determined by the placement of the load application strips. The focus of the presented investigations was the examination to what extent the splitting tension tests

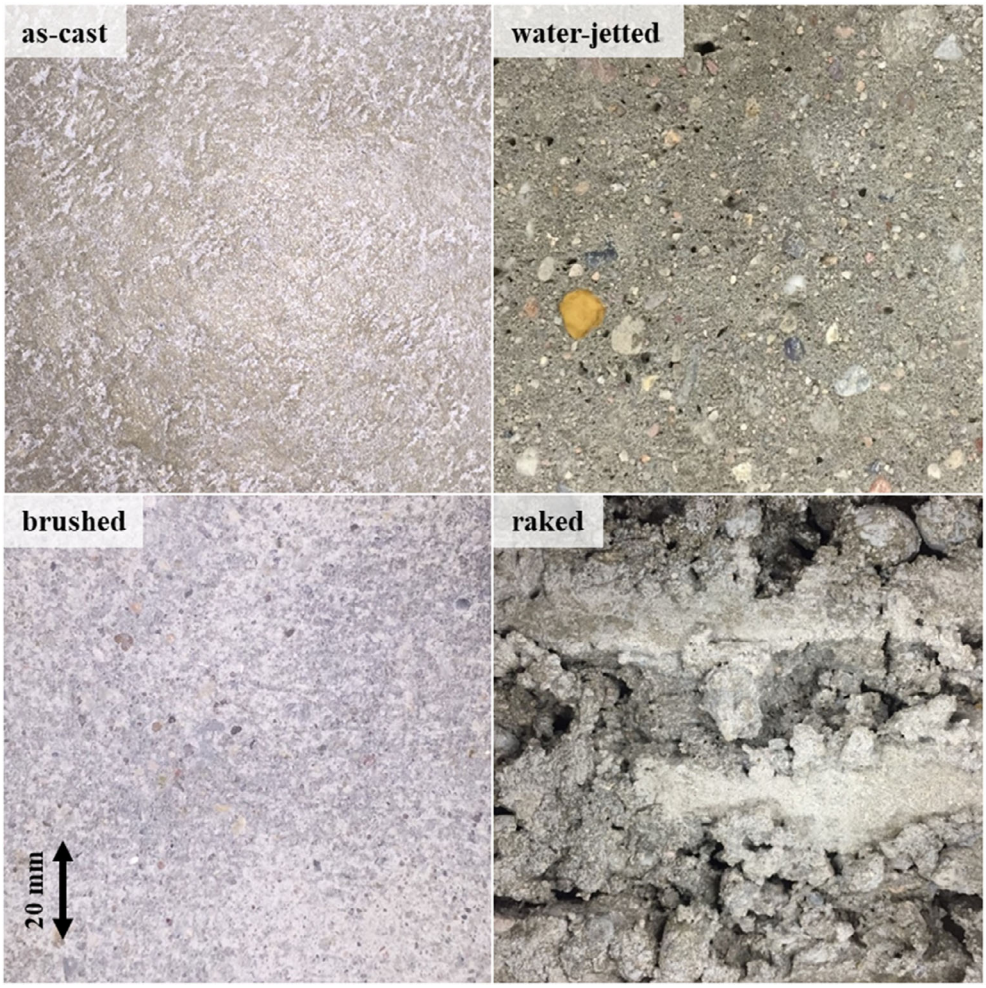

FIGURE 1 Interfaces after different treatment of as-cast, water-jetted, brushed, and raked joints prior to addition of the second concrete layer

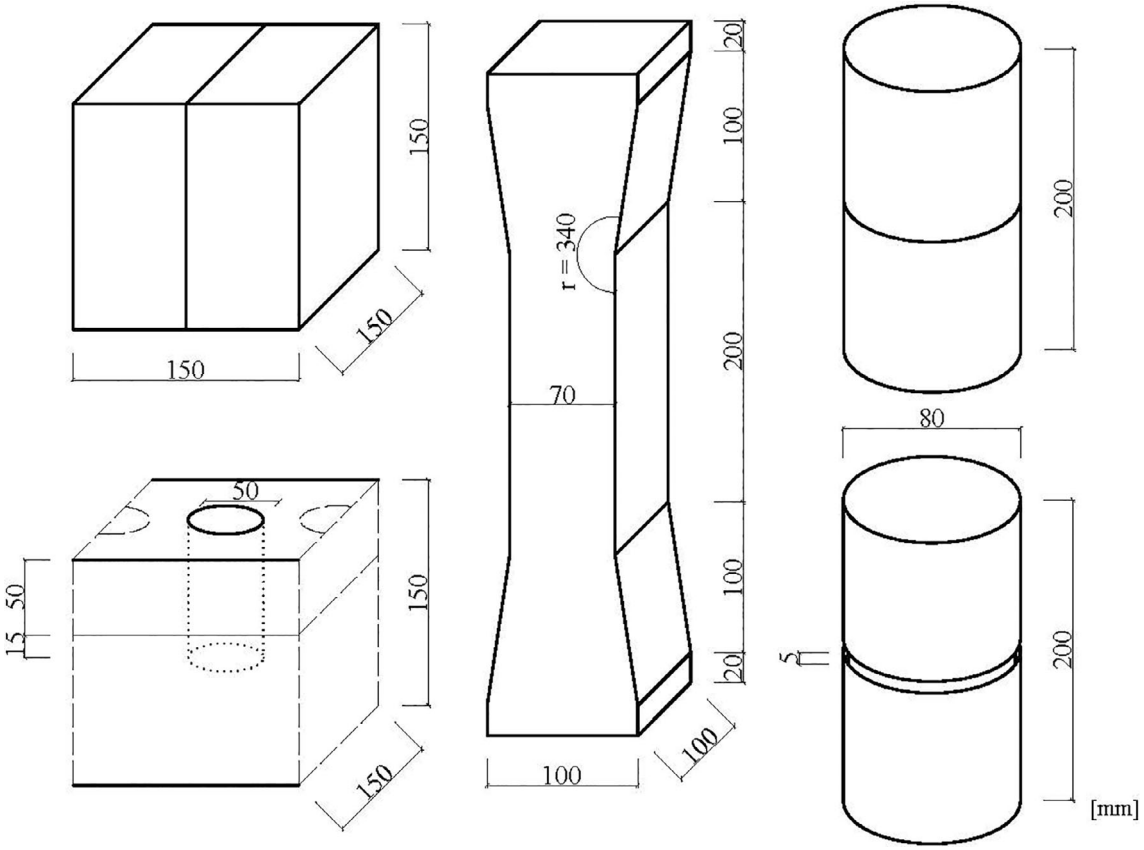

FIGURE 2 Specimen geometry for splitting tension tests (top left), pull-off tests (bottom left), and direct tension tests (mid and right)

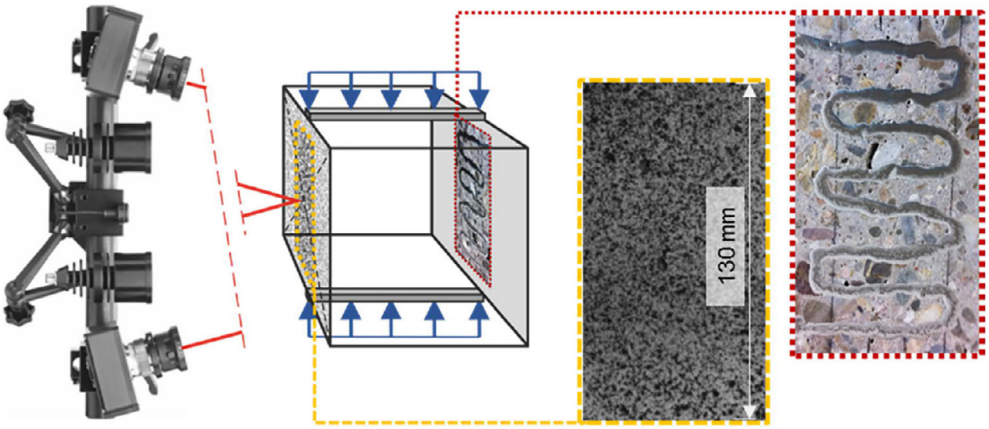

FIGURE 3 Schematic representation of the splitting device with ARAMIS camera system (left) with stochastic spray pattern on the surface of the specimens (middle) and conductive silver paint as trigger on the back (right)[34]

are suitable for determining the uniaxial tensile strength of construction joints. This question arises from the overestimation of the actual splitting tensile strength of construction joints described in various studies.[6,14]

For this purpose, test specimens with three different joint preparation methods (as-cast (a), water-jetted (w), and raked (r)) as well as monolithic specimens (m) were produced. The rake-pattern was perpendicular to the direction of the compressive load. Four different geometries were investigated for detecting a possible size effect: cubes with edge lengths of 200 mm (labeled c200) and 150 mm (c150), respectively, and quadratic prisms sawn from 150 mm cubes with a thickness of 75 mm and 50 mm (p75 and p50). Moreover, the splitting tension test was implemented with two different load distribution strips. In addition to the hard fiber strips specified in EN 12390-6:2010–09,[23] steel strips with a cross-section of 15×15 mm^2 were used to analyze the influence of load application strips with higher modulus of elasticity.

Figure 3 depicts the general splitting tension test setup. Specimens were installed in the testing machine in such a way that the construction joint was parallel to the

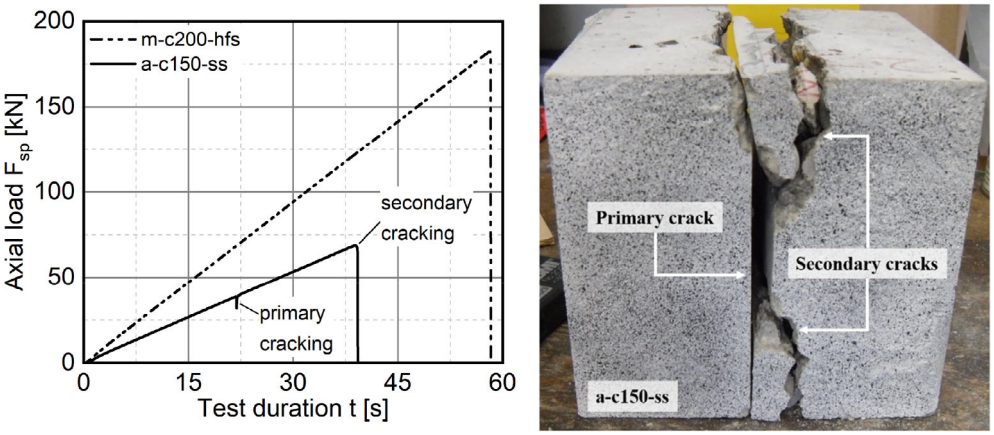

FIGURE 4 Results of splitting tension test. Left: Exemplary load–time-diagrams for a monolithic cube with an edge length of 200 mm tested with hard fiber strips (m-c200-hfs) and a cube with as-cast joint with an edge length of 150 mm tested with steel strips (a-c150-ss). Right: Photo of specimen a-c150-ss after testing

direction of pressure and thus normal to the main tensile stress between the load application strips, so that this led to failure in the joint. For the analysis of crack formation using the ARAMIS measuring system of the Society for Optical Measuring Technology (GOM),[24,25] the front of each specimen was painted white and then sprinkled with black spray paint, thus creating a fine stochastic pattern. This enabled the deformations on the sample surface to be recorded and calculated, and based on this, the course of the crack formation could be examined. The recording took place over a period of 3 s with a measurement rate of 340 Hz. The fracture process in splitting tension tests on low-strength concretes takes about 1.6–2.0 ms.[3] In order to optimally record the time period of the crack formation with the ARAMIS camera system, a trigger was installed on the sample in the form of a brittle conductive silver lacquer, which was applied over the joint on the back of the sample. As soon as a crack started to form in the concrete, the conductive silver lacquer also cracked, causing an applied electric current to drop and transmit a signal to the ARAMIS system. From the ARAMIS ring buffer, 680 images were saved before the trigger signal was received and 340 images afterwards.

In addition to crack formation, the complete development of the axial load F_{sp} was recorded for each splitting tension test. The load rate was set to $\frac{d\sigma_{ct,sp}}{dt} = 0.05 \frac{MPa}{s}$, according to EN 12390-6:2010-09.[23] The splitting tensile stress $\sigma_{ct,sp}$ was calculated from Equation (1), where l [mm] is the length of the contact zone between the test specimens and the load application strips and d [mm] is the cross-section dimension.

$$\sigma_{ct,sp} = \frac{2 * F_{sp}}{\pi * l * d}. \quad (1)$$

EN 12390-6:2010-09[23] subsequently defines the splitting tensile strength $f_{ct,sp}$ as the maximum of $\sigma_{ct,sp}$, assuming cracking and specimen failure at the highest load reached during a splitting tension test. The evaluation of the present splitting tension tests yielded two characteristic loading curves, which are depicted in Figure 4. The first type of curve shows a continuously increasing load and an abrupt decrease to zero at the supposed specimen failure, which was observed for monolithic specimens and raked joints. Specimens with water-jetted or as-cast joints behaved in a similar way, but often showed a small and time-limited force-reduction before reaching the maximum load. By comparing load curves and ARAMIS data, the reason for the observed behavior was investigated. Figure 5 shows an exemplary crack formation of a monolithic specimen. The unloaded test specimen is shown on the left without any expansion or deformation (blue). As the load on the distribution strips increases, so do the strains in the stress plane. These are higher at the center of the specimen than in the load application areas above and below. A narrow crack is already visible in the fourth pair of images, which is shown as a strongly stretched (red) area in the ARAMIS output. The two pairs of images on the right show the separating crack and finally the complete failure of the test specimen. The entire depicted cracking process lasted about 15 ms.

Accordingly, two types of cracking could be identified from the evaluation of the optical measurements: primary cracking beginning at the center of the specimen, which triggered the ARAMIS measurement, and secondary cracking at the load distribution strips (see Figure 5). For the specimens with a strong bond (m, r), only the secondary crack lead to the failure of a specimen. In the case of samples with a weaker bond (w, a) a primary crack often occurred significantly before the final failure of the samples. In case of the specimens with the water-jetted joint, the formation of the separating crack was even clearly audible during the test, allowing it to be easily assigned to the decrease in the test data. After a further

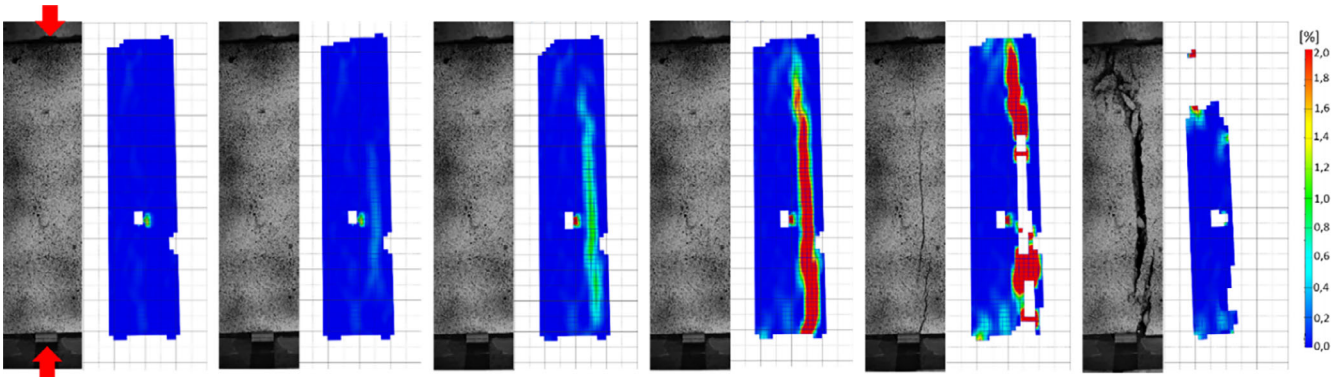

FIGURE 5 Fracture process and ARAMIS data including local strain [%] for a monolithic specimen (m-c200-hfs)

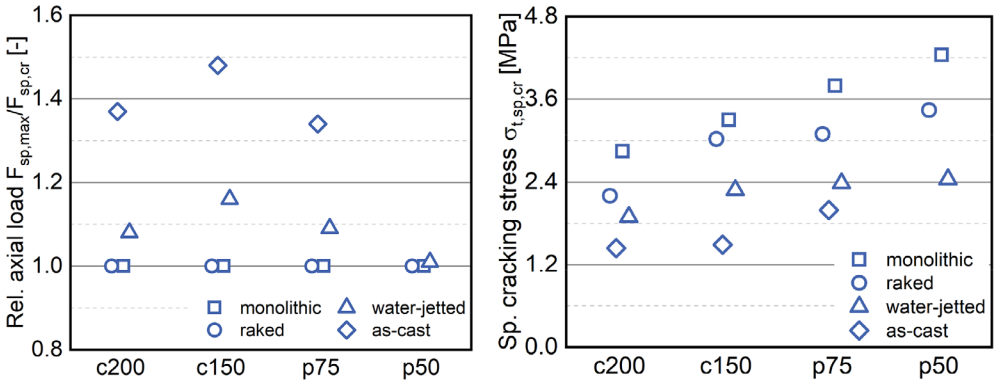

FIGURE 6 Ratio of the axial force at primary cracking $F_{sp,cr}$ and the maximum axial force at secondary cracking $F_{sp,max}$ for the investigated joint preparation methods and specimen geometries (left) and the related stresses at primary cracking $\sigma_{t,sp,cr}$ (right). Averages of two tests with hard fiber load distribution strips. See Section 3 for series labels

increase of the load, the specimens ultimately failed due to the formation of wedges at the load distribution strips because of secondary cracking.

Following the identification of primary and secondary cracking, the ratio of the associated axial forces, $F_{sp,cr}$ and $F_{sp,max}$ as depicted in Figure 6 illustrates the overestimation of the true adhesive strength through the assessment of the maximum axial forces according to EN 12390-6:2010-09[23] especially in the case of joints with weak adhesive bond.

The identification of primary cracking through load–time curves and optical measurements allows a more detailed analysis of the obtained splitting tension test results. With increasing roughness of the construction joints, the splitting tensile strength of the samples also increases. The samples with as-cast joints achieved the lowest values with $\sigma^{a}_{t,sp,cr,150mm} = 1.5$ MPa, followed by the samples with the water-jetted old concrete surface ($\sigma^{w}_{t,sp,cr,150mm} = 2.3$ MPa), where the weak cementitious laitance that is present in as-cast-joints is removed. The raked interfaces yielded the highest values among the composite specimens with $\sigma^{r}_{t,sp,cr,150mm} = 3.0$ MPa, surpassed only by the monolithic samples ($\sigma^{m}_{t,sp,cr,150mm} = 3.3$ MPa). The cause of the increased splitting tensile strength of the rougher surfaces is the enlarged adhesive surface area and the stronger mechanical interlocking between old and new concrete. For raked joints, there is also the fact that the joint width is wider than the area of maximum tensile stress due to the strong roughening of the fresh concrete. The results also showed a pronounced size effect, which is typical for tensile-loaded concrete (Figure 6).

Splitting tension tests using the standardized load distribution strips made of hard fiber yielded higher cracking stresses than steel strips. Presumably, the high stiffness of the steel leads to the development of stress peaks in the specimen and thus to premature failure. In addition, it was observed that cracking often starts at the specimen edge when the load is applied via steel strips. According to the ideal conception of the stresses in the splitting tension test, however, the specimens should begin to crack at the center. This observation can also be explained by an unfavorable influence on the stress distribution in the edge area of the test specimen by the use of the steel strips, thus affirming similar previous observations.[6,14]

4 | DIRECT TENSION TESTS

For direct tension tests, drill-cores with a diameter of 80 mm were taken from concrete cubes ($l = 200$ mm) and tested between 27 and 30 days after casting the

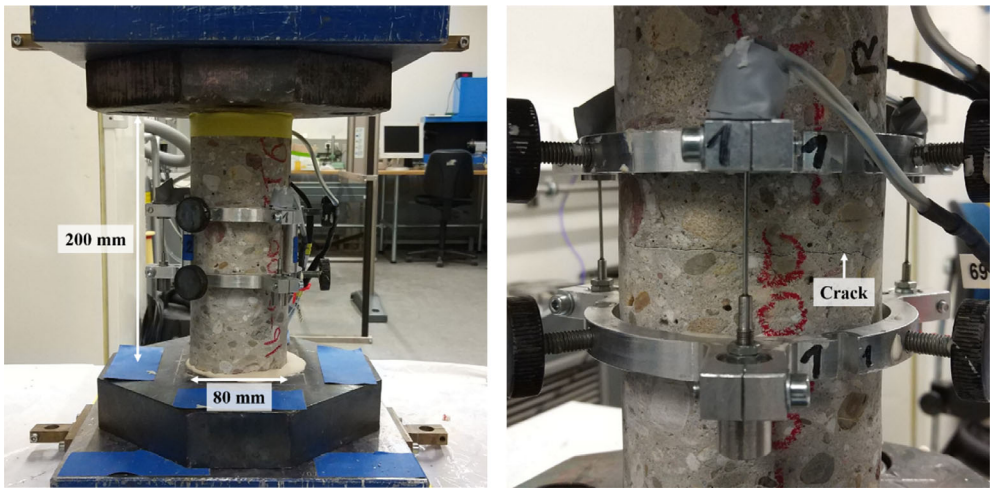

FIGURE 7 Direct tension test setup on a specimen with a raked joint before load application (left) and after cracking (right) at KIT-IMB/MPA

second layer. Joints were located at half the cylinder height. Due to the elaborate and time-consuming setup, only specimens with brushed and raked interfaces in addition to monolithic specimens were investigated. As the joints provide a structural weakness which localizes cracking, deformations w could be measured with three inductive displacement sensors and a measuring length of $l_0 = 50$ mm. For predefining crack initiation in monolithic cylinders, a notch with a depth of 6 mm had to be cut into each specimen. The uniaxial tensile strength of concrete without joints was also measured on bone-shaped specimens, which were equipped with six inductive displacement sensors covering a measuring length of $l_0 = 250$ mm (see Figure 1 for geometries).

Before starting the deformation-controlled tension test, each specimen was glued to the load introduction panels with an epoxy resin and left to harden for 20 min under a small compressive load. Deformation was then applied with a constant rate of $\frac{dw}{dt} = 0.5\,\frac{\mu m}{s}$. Tensile forces F_t and deformations w were recorded at 25 Hz. Figure 7 depicts the direct tension test setup. For the description of tensile behavior, three characteristic parameters were analyzed: tensile strength f_{ct}, secant modulus of elasticity $E_{ct,S}$, and fracture energy G_F. Tensile strength was obtained from monolithic bone-shaped specimens and jointed cylinders. Only tests where cracking occurred in the joint or in the measuring range of monolithic specimens were used, thereby ensuring uniform uniaxial tensile stresses. The net tensile strength of notched monolithic specimens $f_{ct,n}$ was obtained by replacing the specimen cross-section area fracture A_c by the ligament area $A_{c,n}$ in Equation (2).

$$f_{ct} = max\,\sigma_t = max\,\frac{F_t}{A_c}. \tag{2}$$

From a micromechanical point of view, the modulus of elasticity should be determined as slope of the tangent to the stress–strain curve at $\sigma_t = 0$, which is often unfeasible for metrological reasons. Since stress–strain curves for concrete are approximately linear for low stresses, the modulus of elasticity can instead be obtained as secant modulus of an upper stress σ_a and the corresponding strain $\varepsilon(\sigma_a)$. Rostásy et al.[26] propose $\sigma_a = 1/3 \times f_{ct}$, which was adopted for the presented research with the addition of a lower boundary at $\sigma_b = 1/20 \times f_{ct}$ for eliminating any setting effects (Equation (3)). $E_{ct,S}$ for notched monolithic specimens was calculated on the basis of volumetrically averaged stresses, thereby disregarding distortions through stress concentrations. The secant modulus can also be used for assessing elastic behavior. In a linear-elastic material, $E_{ct,S}$ is independent of σ_a. The present research introduces a coefficient of linearity L describing the ratio of two secant moduli determined for $\sigma_a = 1/3 \times f_{ct}$ and $\sigma_a = 1/6 \times f_{ct}$, respectively.

$$E_{ct,S} = \frac{\sigma_a - \sigma_b}{\varepsilon(\sigma_a) - \varepsilon(\sigma_b)}. \tag{3}$$

The fracture energy G_F is the energy per unit area required for a separating crack and can be illustrated as the area under the stress–deformation curve (Equation (4)). This involves executing time-consuming tests until tensile stresses reduce to zero. In the present study, tensile-softening behavior was analyzed up to a deformation of $w_u = 0.3$ mm. Any extrapolation (e.g.,[2]) was foregone.

$$G_F = \int_0^{w_u} \sigma_t(w)dw. \tag{4}$$

Due to the brittle tension-softening behavior of concrete and especially of concrete joints, so-called snap-backs can occur when elastic resilience exceeds the crack opening displacement resulting in unsteady stress–deformation curves. Examples of stress–displacement curves with varying snap-back magnitude are given in Figure 8. While snap-backs only affected small segments (if any) of stress–deformation curves of monolithic concrete, specimens with as-cast joints turned out to be highly brittle and proved problematic for the assessment of the tension-softening behavior. On tests without snap-back it was found that a single-parameter hyperbolic fit yields a satisfying approximation to the tension-softening curve, in contrast to exponential functions,[27–29] which tend to overestimate the measured stresses. Thus, in case of a snap-back tension-softening curves were interpolated using Equation (5).

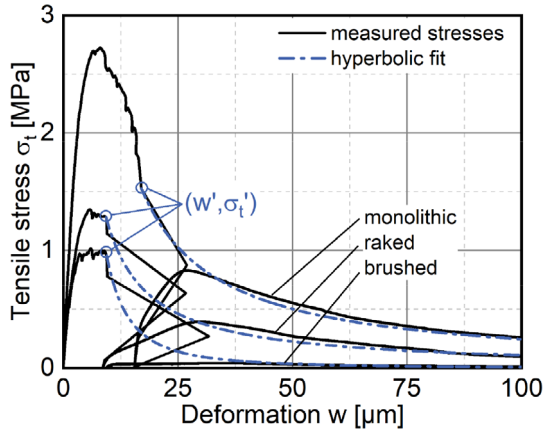

FIGURE 8 Stress–deformation curves of three exemplary direct tension tests showing snap-backs and respective hyperbolic fit-curves

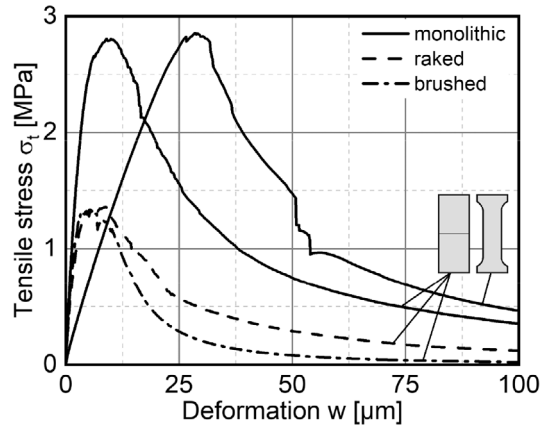

FIGURE 9 Average stress–deformation curves of direct tension tests for different joint types and geometries

$$\sigma_{t,h}(w) = \sigma_t' * \left(\frac{w'}{w}\right)^p, \tag{5}$$

with p the fit parameter.

The ultimate measured values before each snap-back, w' and σ_t' were used as anchor-point of the hyperbole and the parameter p was determined by fitting the hyperbole to the measured values following snap-back by means of the least-squares method. In case of a snap-back, G_F was obtained from measured $\sigma_t(w)$ for $w \le w'$ and $\sigma_{t,h}(w)$ for $w' \le w \le w_u$.

The results from direct tension tests are presented in Figure 9 and Figure 10. All 12 tests on cylinders showed the desired cracking in the joint or notch, respectively. Two bone-shaped specimens failed outside the desired area, which is why two additional specimens were tested to achieve four evaluable tests.

Monolithic specimens show a similar tensile strength despite different geometries. This can be attributed to two phenomena of fracture mechanics: due to stress concentrations at the notch root the net tensile strength of notched specimens usually underestimates the "real" tensile strength. At the same time, tensile strength underlies a considerable size effect, where the probability of a local imperfection leading to crack induction rises with greater specimen dimensions, resulting again in strength reduction, thus impeding the comparison of tension test results of specimens with different geometries. However, in monolithic specimens a reduction of the cross-section area either in the form of a notch or a bone-shaped specimen is essential for preventing cracking due to multi-axial stresses at load application. Results show that this measure can be foregone for specimens with joints, as these present a structural weakness sufficient for impeding crack formation elsewhere.

The determination of the secant modulus of elasticity is possible for the investigated specimen types, with jointed specimens yielding lower secant moduli than bone-shaped monolithic specimens, especially in the case of raked joints, where the disrupted volume cannot be neglected. Since the coefficient of linearity for raked joints is lowest with $L = 86\%$, compared to 93% for both brushed joints and monolithic bone-shaped specimens, this behavior can be explained by local stress concentrations at the joint resulting in deviations from Hooke's law. Similar observations can be made for notched monolithic specimens with $L = 89\%$.

In contrast to tensile strength and secant modulus, fracture energy of monolithic concrete needs to be obtained from notched specimens, where crack

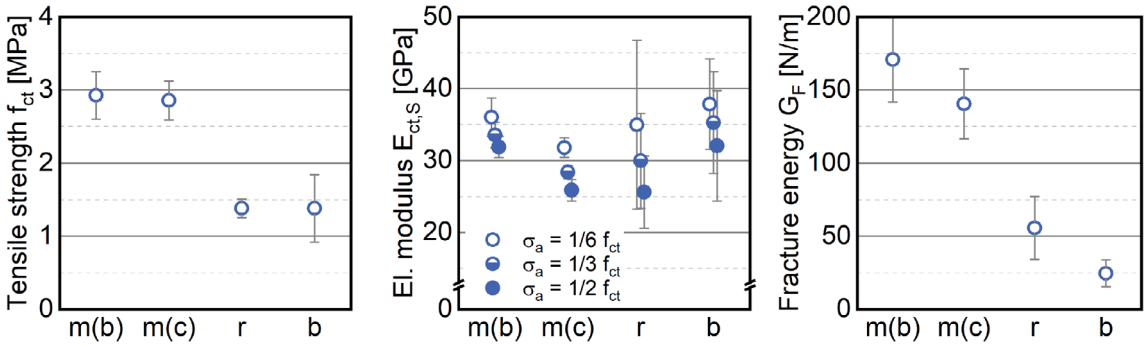

FIGURE 10 Average direct tensile strength f_{ct} (left), secant moduli of elasticity $E_{ct,S}$ for different upper stress boundaries (mid), and specific fracture energy G_F (right) of bone-shaped or notched cylindrical monolithic (m(b)/m(c)) and jointed (r/w) specimens

formation is predefined. Due to stress concentration, the formation of a localized single crack can be assumed. Bone-shaped specimens yield a higher fracture energy, as dispersed micro-cracks form before a singular separating macro-crack, leading to an unquantifiable surface area. Tension-softening behavior mainly depends on aggregate interlock, which again correlates with crack path roughness. In monolithic normal strength concrete, the interfacial transition zone (ITZ) between hardened cement paste and aggregates presents a structural weakness where cracks usually form. Thus, the crack path and subsequently the fracture energy depend on geometrical properties of the aggregates.

Concrete joints act accordingly like the ITZ between hardened cement paste and aggregate but have a predefined crack path. It can generally be assumed that regardless of surface preparation cracked concrete joints exhibit a lower roughness than cracks in monolithic concrete—if joints were rougher, cracks would propagate through paste-aggregate-ITZ instead of joint interface Therefore, the fracture energy of a concrete joint cannot exceed the fracture energy of the surrounding concrete except for statistical reasons.

Results from direct tension tests generally exhibit a high scatter for tensile strength, secant modulus of elasticity, and specific fracture energy, with increasing magnitude, as indicated by variation coefficients in Figure 10. Scatter of the results for monolithic concrete appear to be independent on specimen geometry, which does not agree with size-effect theory. Variation coefficients for concrete joint tensile strength and fracture energy, however, are much higher with the single exception of the tensile strength of raked cylinders, despite all specimens originating from same batch and receiving the same surface treatments. This illustrates that for the development of a structural design model for concrete joints, an even higher amount of tests is required, compared to monolithic concrete.

5 | PULL-OFF TESTS

Pull-off tests were executed based on EN 1542:1999-07[30] with minor deviations. Various interface parameters were chosen to analyze the influence of surface preparation on the bond strength of concrete layers, with the main focus of the first five series lying on mechanical roughening (as-cast, wire-brushed, water-jetted, raked) and the comparison to monolithic concrete without a joint. Based on wire-brushed joints, two alterations of the usual procedure, where the second layer was added following a storage for 7 days under wet burlap sacks, were realized with regard to concrete age (6 h (bt1) or 28 days (bt2)) and moisture saturation (storage under water after demolding the first layer (bs1) or additional moistening immediately before casting the second layer (bs2)), totaling in nine different interface parameters. For each parameter, one concrete beam with the dimensions 700 mm × 150 mm × 150 mm was produced. Specimens were jointed horizontally at 2/3 of the total beam height, resulting in an overlay thickness of 50 mm. Into each beam, a total of nine cores with a diameter of d_p = 50 mm were predrilled with a diamond drill to a depth of 65 mm to increase the chances of a failure within the interface. The increased number of drill-cores within one beam was realized by neglecting the required minimum distance between cores specified in EN 1542:1999-07.[30] However, as preliminary tests had shown no adverse effects, the impact of the reduced distance was deemed insignificant in favor of a larger number of results.

The testing method is based on a principle, in which a steel adapter is bonded onto the specimen surface, while a uniaxial tensile force is steadily applied to determine the joint bond strength. The steel adapters used for the tests present a diameter of 50 mm and a minimum thickness of 20 mm, in order to allow for a uniform load

introduction. Prior to attaching an adapter, the core surface was cleaned with a wire brush, thus removing the weakened cementitious laitance layer. A two-component epoxy bonding agent was subsequently applied evenly onto the core surface. After centering the adapters, the adhesive was left to dry and harden for a minimum of 1 h at room temperature. Due to the reduced spacing of the drill-cores, testing of each beam was split into two intervals. Figure 11 shows the test setup.

The pull-off apparatus was sequentially placed perpendicularly over each core sample. Apparatus and sample were connected through a spherical bearing to ensure a uniaxial load introduction. The load rate was set to 600 N/s, equivalent to the direct tension tests. The maximum applicable force F_h was recorded and converted to a value for pull-off strength f_h using Equation (6).

$$f_h = \frac{4 * F_h}{\pi * d_p^2}. \quad (6)$$

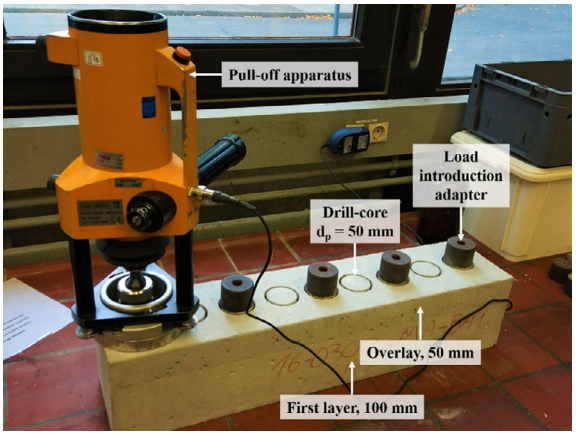

FIGURE 11 Pull-off test setup at the beginning of the first interval

Results from the experimental investigation presented four possible failure modes. While failure mostly occurred in the interface, three further failure modes shown in Figure 12 underline a certain unreliability, which is affiliated with the simple testing method. It is crucial for the failure to occur at the joint, in order to estimate the interfacial bond strength with the pull-off test.

A failure in the interface demonstrates an adhesive failure at the specified weakened locality and f_h can be interpreted as the tensile bond strength. Due to material heterogeneity, a cohesive failure outside of the interface is not completely inevitable, in which case the pull-off strength can only serve as a lower boundary of the tensile bond strength. Failure outside of the interface implies the joint presenting a greater tensile strength than the concrete itself, which is unlikely. A reoccurring cause for this phenomenon is the localization of aggregates, which evokes unwanted stress peaks at crack initiation. In the present research, a strength measurement affiliated with a failure outside of the interface was deemed unusable for the evaluation of bond strength. For this reason, the number of specimens was increased to nine, compared to five required by EN 1542,[30] to gain a larger sampling

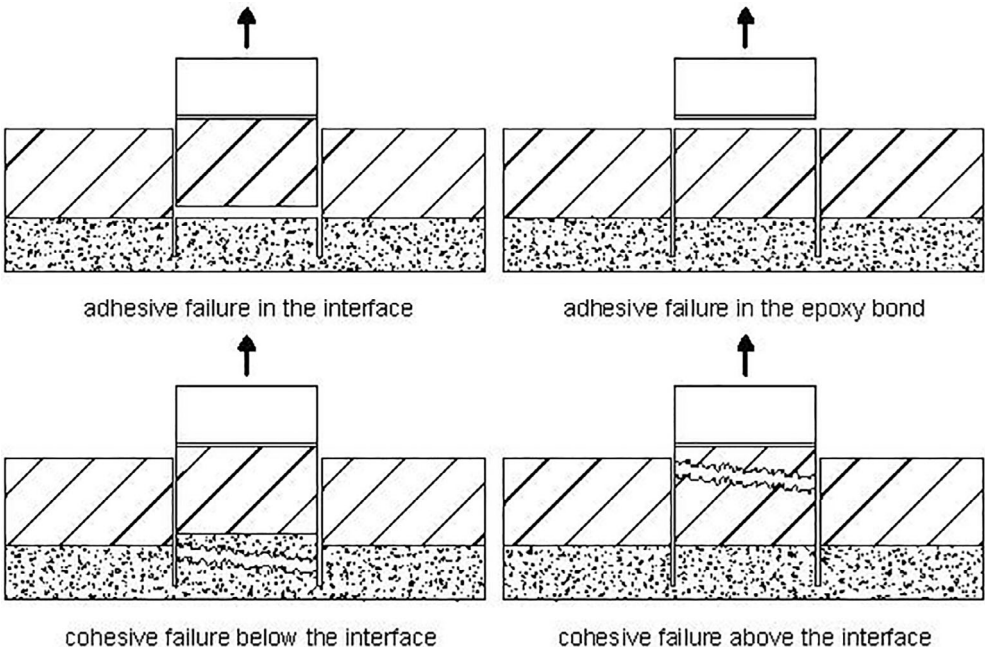

FIGURE 12 Failure modes in pull-off tests

pool. A result was only taken into consideration when the crack path ran at least partially through the interface.

From the 72 pull-off tests on jointed specimens, a total of 50 showed adhesive failure, with 6 and 15 specimens failing below or above the interface (one failure of the epoxy). The proportion of specimens with cohesive failure increases with higher pull-off strength, as labeled in Figure 13. An overall comparison of the results shows that the measured pull-off strength varies strongly even though the specimens were pulled from the same beam. In case of combined adhesive and cohesive failures within one beam, calculated pull-off strengths are similar regardless of failure mode, with cohesive failure showing an even greater scatter. This impedes the determination of plausible average values for the interface bond strength.

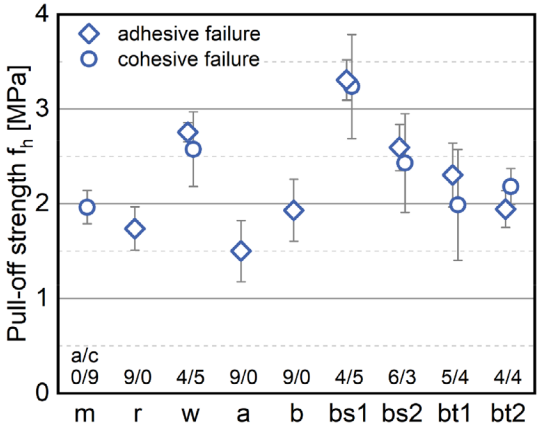

FIGURE 13 Average pull-off strength for the investigated joint preparation methods. Labels indicate the number of specimens with adhesive/cohesive failure

Specimens with as-cast joints exhibit the lowest bond strength. An increase is witnessed once the joint is treated mechanically. The introduction of a rake pattern increases surface roughness and aggregate interlock. The removal of the laitance layer via wire brush or especially water-jetting by increased interfacial cleanliness and partial exposure of aggregates yields further increase in strength. Furthermore, the implementation of water-jetting shortens the length of unwanted superficial micro cracks, which decreases the probability of failure caused by stress concentration at the crack tip.[31]

Elevated values of bond strength could also be measured on specimens where the substrate surface was moistened with a sponge prior to adding the concrete overlay. The results of saturated specimens are questionable, as higher than expected bond strengths, exceeding the concrete tensile strength according to EN 12390-6[23] were measured. The present results also disagree with results from past research, where it was established that the saturation of the substrate surface results in lower bond strengths between substrate and overlay.[32,33] The variation of concrete age of the first layer does not yield significant deviations.

TABLE 2 Overview of the advantages and disadvantages of different tension test setups for the determination of interfacial adhesive strength

Setup (see Figure 2)	Direct tension	Pull-off	Splitting tension
		Bulk concrete	
Stress state	Tension	Tension	Tension-compression
Requirements on test device	Challenging and expensive frame and device	Specialized device	Standard compressive test setup
Specimen preparation	Limited by load introduction and crack predetermination	Limited by overlay thickness	Variety of specimen geometries possible
Specimen preparation	Extensive	Extensive	Undemanding
Test execution	Slow	Fast	Fast
Recommended number of specimens	Depends on specimen preparation	High	Small
Material properties	$f_{ct}, f_{ct,n}, E_c, G_f$	f_h	$f_{ct,sp}$
Investigation of size effect	Limited by test setup	Possible, but uncommon	Suitable
		Interfaces	
Specimen preparation	Reduced (interfaces predetermine cracking)	Higher (drilling can induce cracks)	Higher (extensive joint alignment)
Change of applicability	Simplified	More suitable	Applicability remains disputed
Recommendation ranking	1	2	3

The pull-off tests fail to produce reasonable results for monolithic concrete. The obtained results are considerably lower than the concrete tensile strength according to EN 12390-6:2010-09[23] and also the direct tensile strength, despite size-effect theory predicting higher strength with smaller specimen dimensions. Moreover, it remains unclear why the results for cohesive failure of jointed specimens are consistently similar to the respective adhesive bond strength, thus exceeding the pull-off strength of monolithic concrete.

6 | CONCLUSION

The determination of the tensile bond strength of concrete joints can be crucial for the evaluation of concrete structures and repair and retrofitting measures. Tension tests generally require standardized setups for obtaining reproducible and reliable results. Different test setups highlight various technical possibilities, but are each afflicted with individual flaws, which require attention when selecting or comparing methods. Due to their lowered strength and pronounced brittleness, as well as limited positioning possibilities, tension testing of concrete joints requires additional consideration.

The splitting tension test can be carried out in common compressive testing machines, which allows a simple realization. For being an indirect test method, splitting tensile test results need conversion into uniaxial tensile strength. Details of this conversion have been thoroughly investigated, but their applicability for concrete joints remains unproven. Moreover, especially for low-strength joints, the interpretation of present results calls for increased attention when specimen halves are able to carry compressive loads even after a tensile failure of the bond, thus opposing the simple practicability. Finally, splitting tension tests require the exact alignment of joint and load introduction, thereby complicating specimen preparation from existing structures. Splitting tension tests should therefore only serve for qualitative laboratory analyses, which is often sufficient for the determination of a relative tensile bond strength compared to monolithic concrete.

In contrast to splitting tension tests, direct tension tests are costly but allow for the determination of the secant modulus of elasticity, tensile strength, and fracture energy from the same specimen. The structural weaknesses presented by joints facilitate test execution, as the crack path is predetermined. Direct tension tests on plain monolithic concrete require the introduction of a notch for crack predetermination or an increased number of tests for obtaining a sufficient amount of usable results. On the other hand, recording the tension-softening curve of concrete joints is prone to measurement errors due to elastic resilience encountering high brittleness. Joint and load alignment is also crucial for a viable test execution. Direct tension test can even be carried out on samples obtained from existing structures, where joints usually run parallel to external surfaces, thus favoring stress application. This is also exploited by pull-off tests, which can be executed in-situ, but only yield the joint tensile strength. The pull-off tests presented in this paper, however, yielded inconclusive results, with regard to monolithic concrete. For both direct tension and pull-off tests, specimen preparation is an issue since drilling or cutting may further impede an already weak adhesive bond, resulting in often untraceable measurement artifacts.

In conclusion, all three tension test setups used in this paper can provide meaningful results but require special attention to specimen preparation and the evaluation of cracking. Table 2 gives an overview of the advantages and disadvantages of different tension test setups for the determination of interfacial adhesive strength. For the evaluation of existing structures, laboratory direct tension tests can provide robust results for adhesive strength, which can be coupled with in-situ pull-off tests. The simplicity of splitting tension tests—despite requiring stress conversion—is mitigated by the need for joint alignment, in contrast to direct tension tests, where the structural weakness provided by the joint is beneficial for test execution.

FUNDING

Federal Ministry for Digital and Transport: BMVI-Expertennetzwerk Wissen - Können - Handeln, Grant Number: B3951.03.04.70014.

DATA AVAILABILITY STATEMENT

The data that support the findings of this study are available from the corresponding author upon reasonable request.

ORCID

Jan P. Höffgen https://orcid.org/0000-0003-1115-282X

REFERENCES

1. Mechtcherine V. Bruchmechanische und fraktologische Untersuchungen zur Rissausbreitung in Beton. Dissertation. Karlsruhe: Universität Karlsruhe; 2000 (in German).
2. Kessler-Kramer C. Zugtragverhalten von Beton unter Ermüdungsbeanspruchung. Dissertation. Karlsruhe: Universität Karlsruhe; 2002. http://digbib.ubka.uni-karlsruhe.de/volltexte/20522002 (in German).
3. Malárics V. Ermittlung der Betonzugfestigkeit aus dem Spaltzugversuch an zylindrischen Betonproben, Dissertation. Karlsruhe: Karlsruher Institut für Technologie; 2011 (in German).

4. Saouma VE, Broz JJ, Brühwiler E, Boggs HL. Effect of aggregate and specimen size on fracture properties of dam concrete. J Mater Civ Eng. 1991;3(3):204–18. ISSN 0899-1561.
5. Tschegg EK, Ingruber M, Surberg CH, Münger F. Factors influencing fracture behavior of old-new concrete bonds. ACI Mater J. 2000;97(4):447–53.
6. Lenz P. Beton-Beton-Verbund: Potentiale für Schubfugen. Dissertation. München: Technische Universität München; 2012 (in German).
7. Randl N, Steiner M, Peyerl M. Hochfester Aufbeton zur Tragwerksverstärkung. Teil 1: Kleinkörperversuche. Beton- und Stahlbetonbau. 2020;115(2):106–16. https://doi.org/10.1002/best.201900028 (in German).
8. Hillerborg A. The theoretical basis of a method to determine the fracture energy gf of concrete. Mater Struct. 1985;18(4):291–6. https://doi.org/10.1007/BF02472919
9. Abu-Tair AI, Rigden SR, Burley E. Testing the bond between repair materials and concrete substrate. ACI Mater J. 1996;93(6):553–8.
10. Farzad M, Shafieifar M, Azizinamini A. Experimental and numerical study on bond strength between conventional concrete and ultra high-performance concrete (UHPC). Eng Struct. 2019;186:297–305. https://doi.org/10.1016/j.engstruct.2019.02.030
11. Zega BC, Prayuda H, Monika F, Saleh F, Wibowo DE. Effects of cold joint and its direction on the compressive and flexural strength of concrete. Int J GEOMATE. 2021;20(82):86–92. https://doi.org/10.21660/2021.82.J2086
12. Geissert DG, Li S, Franz GC, Stephens JE. Splitting prism test method to evaluate concrete-to-concrete bond strength. ACI Mater J. 1999;96(3):359–66. https://doi.org/10.14359/634
13. Momayez A, Ehsani MR, Ramezanianpour AA, Rajaie H. Comparison of methods for evaluating bond strength between concrete substrate and repair materials. Cem Concr Res. 2005. ISSN 00088846;35(4):748–57. https://doi.org/10.1016/j.cemconres.2004.05.027
14. Müller AJ. Zum Zug- und Schubtragverhalten von Betonfugen. Dissertation, München: Technische Universität München; 2009 (in German).
15. Santos PMD, Júlio ENBS. Recommended improvements to current shear-friction provisions of model code. In: International Federation for Structural Concrete, editor. 3rd fib international congress. Proceedings of a meeting held 29 May–2 June 2010, Washington, DC, USA. Washington, DC: Precast Prestressed Concrete Institute (PCI); 2010.
16. Zanotti C, Randl N. Are concrete-concrete bond tests comparable? Cem Concr Compos. 2019. ISSN 09589465;99:80–8. https://doi.org/10.1016/j.cemconcomp.2019.02.012
17. Hu B, Meng T-F, Li Y, Li D-Z, Chen L. Dynamic splitting tensile bond behavior of new-to-old concrete interfaces. Constr Build Mater. 2021. ISSN 09500618;281:122570. https://doi.org/10.1016/j.conbuildmat.2021.122570
18. Austin S, Robins P, Pan Y. Tensile bond testing of concrete repairs. Mater Struct. 1995;28:249–59.
19. Santos PMD, Júlio ENBS, Silva VD. Correlation between concrete-to-concrete bond strength and the roughness of the substrate surface. Constr Build Mater. 2007. ISSN 09500618;21(8):1688–95. https://doi.org/10.1016/j.conbuildmat.2006.05.044
20. Silfwerbrand J. Shear bond strength in repaired concrete structures. Mater Struct. 2003;36(6):419–24. https://doi.org/10.1007/BF02481068
21. Beushausen H. Long-term performance of bonded concrete overlays subjected to differential shrinkage. Dissertation. Cape Town: University of Cape Town; 2005.
22. EN 12390-3:2019-10. Testing hardened concrete – Part 3: Compressive strength of test specimens; German version EN 12390-3:2019. 2019.
23. EN 12390-6:2010–09. Testing hardened concrete – Part 6: Tensile splitting strength of test specimens; German version EN 12390-6:2009. 2010.
24. GOM mbH. ARAMIS Benutzerhandbuch Software. Braunschweig, 2007 (in German).
25. GOM mbH. ARAMIS Benutzerinformation – Hardware. Braunschweig, 2008 (in German)
26. Rostásy FS, Warnecke P, Pusch U. Zugfestigkeit von Konstruktionsleichtbeton und Normalbeton bei sehr tiefen Temperaturen. Braunschweig: Institut für Baustoffe, Massivbau und Brandschutz IBMB; 1988 (in German).
27. Gopalaratnam VS, Shah SP. Softening response of plain concrete in direct tension. ACI J Proc. 1985;82(3):310–23. https://doi.org/10.14359/10338
28. Cornelissen HAW, Hordijk DA, Reinhardt HW. Experimental determination of crack softening characteristics of normalweight and lightweight concrete. Heron. 1986;31(2):45–56.
29. Duda H. Bruchmechanisches Verhalten von Beton unter monotoner und zyklischer Zugbeanspruchung, Volume 419 of Deutscher Ausschuss für Stahlbeton. Beuth, Berlin: DAfStb; 1991. https://doi.org/10.2366/3707163 ISBN 9783410656197 (in German).
30. EN 1542:1999-07. Products and systems for the protection and repair of concrete structures – Test methods – Measurement of bond strength by pull-off; German version. EN 1542:1999. 1999.
31. Courard L, Bissonnette B, Belair N. Effect of surface preparation techniques on the cohesion of superficial concrete: comparison of jack-hammering and waterjetting. In: Alexander MG, Beushausen H-D, Dehn F, Moyo P, editors. Concrete repair, rehabilitation and retrofitting, Balkema - Proceedings and monographs in engineering, water and earth sciences. Leiden: Taylor & Francis/Balkema; 2006. p. 1027–31 ISBN 0415396549.
32. Silfwerbrand J. Bonded concrete overlays - research needs. In: Marchand J, editor. 2nd international RILEM symposium on advances in concrete through science and engineering, Québec, Canada. Bagneux: RILEM Publications; 2006. p. 193–206, Bagneux, France.
33. Saucier F, Pigeon M. Durability of new-to-old concrete bondings. In: Malhotra VM, editor. Evaluation and rehabilitation of concrete structures and innovations in design: SP-128. Volume 1. Farmington Hills, MI: American Concrete Institute; 1991. p. 689–705. https://doi.org/10.14359/2066
34. T. Reschke, V. Malárics-Pfaff, H. Fleischer, and J. P. Höffgen. Scherfestigkeit von Beton und Mauerwerk an bestehenden Wasserbauwerken: FuE-Abschlussbericht: BAW-Nr. B3951.03.04.70014. Karlsruhe, 2019 (in German).

AUTHOR BIOGRAPHIES

Jan P. Höffgen, M.Sc., Research Assistant,
Karlsruhe Institute of Technology, Institute of Concrete Structures and Building Materials, Karlsruhe, DE 76131, Germany
Email: hoeffgen@kit.edu

Matthias Mohs, M.Sc., Graduate Student (formerly), Research Assistant (presently),
Karlsruhe Institute of Technology, Institute of Concrete Structures and Building Materials, Karlsruhe, DE 76131, Germany
Federal Waterways Engineering and Research Facility, Structural Engineering, Karlsruhe, DE 76187, Germany
Email: matthias.mohs@baw.de

Eric Sonderegger, M.Sc., Graduate Student (formerly),
Karlsruhe Institute of Technology, Institute of Concrete Structures and Building Materials, Karlsruhe, DE 76131, Germany
Email: sonderegger_eric@yahoo.de

Viktória Malárics-Pfaff, Senior Research Engineer,
Federal Waterways Engineering and Research Facility, Structural Engineering, Karlsruhe, DE 76187, Germany
Email: viktoria.malarics-pfaff@baw.de

Frank Dehn, Professor,
Karlsruhe Institute of Technology, Institute of Concrete Structures and Building Materials, Karlsruhe, DE 76131, Germany
Email: frank.dehn@kit.edu

How to cite this article: Höffgen JP, Mohs M, Sonderegger E, Malárics-Pfaff V, Dehn F. Experimental methods for the analysis of the tensile behavior of concrete joints. Structural Concrete. 2022. https://doi.org/10.1002/suco.202200181